6th ICNTC 2020 Special Issue

J. Indian Chem. Soc.
Vol. 97, October(C) 2020

The Effect of Reaction Temperature and Times on Structural and Magnetic Properties of $Zn_{0.25}Fe_{2.75}O_4$

Gulsum CALISKAN and Nurcan DOGAN*
Department of Physics, Faculty of Science, Gebze Technical University, 41400 Kocaeli, Turkey
*E-mail: nurcandogan80@gmail.com
Manuscript Received online 10/26/2020, Accepted 11/13/2020

The Zinc doped iron oxide nanoparticles were successfully synthesized by hydrothermal process at temperatures of 150 and 180°C for time of 6, 12, and 22h. The average crystallite sizes of the nanoparticles were in the range of 14-24 nm with small size distribution. SEM analysis confirmed that all of $Zn_{0.25}Fe_{2.75}O_4$ nanoparticles show a spherical form. The reaction temperature rise up to 180°C led to the increasing of crystallinity of nanoparticles. All nanoparticles showed a superparamagnetic behaviour at room temperature.

Keywords: Nanoparticles; hydrothermal process; Zn doped iron oxide; XRD; magnetic properties

Introduction

Zinc is one of the commonly used metal dopants into iron oxide due to minimal toxicity. In literature, various synthesis methods have been proposed for producing Zn doped iron oxide and zinc ferrite nanoparticles, such as co-precipitation method, hydrothermal, sol-gel method, thermal decomposition and so on[1-10]. The hydrothermal process is simple and inexpensive in which non-harmful materials are used. The particle size and the magnetic property of nanoparticles can be controlled by arranging the reaction temperature and time, and the other parameters[8]. The goal of this work is to analyze effects of reaction temperature and reaction time on the structural and magnetic properties of the synthesized $Zn_{0.25}Fe_{2.75}O_4$ nanoparticles by using hydrothermal method.

Synthesis of $Zn_{0.25}Fe_{2.75}O_4$ Nanoparticles

The synthesis of sample has been performed by a hydrothermal route. In a typical experimental procedure, 4mmol $FeCl_3.6H_2O$, 1.5mmol $FeCl_2.4H_2O$, 0.5mmol $ZnCl_2$ solutions were dissolved in 40 ml distilled water then into the two necked round bottom flask. The mixture was stirred at 500 rpm for 2 minute under nitrogen gas. After that 5 ml of NH_4OH were dropped to the solution. Then the solution was transferred into the Teflon –sealed autoclave for different temperature and different reaction time, as shown in Table 1. The black precipitates were washed with distilled water in two times and the recent precipitates were dried at 60°C.

Table 1. The hydrothermal conditions used to synthesize $Zn_{0.25}Fe_{2.75}O_4$ nanoparticles

Sample No	Reaction Temperature (°C)	Reaction Time (h)
Sample_1	150	6
Sample_2	150	12
Sample_3	150	22
Sample_4	180	6
Sample_5	180	12

Structural and Phase Analysis Results

To record the structural features of nanoparticles, infrared spectrum measurements were taken using Perkin Elmer Fourier transform infrared spectroscopy between 4000 and 500 cm^{-1}. FTIR spectra of nanoparticles were given in Figure 1. As seen from the spectrum, in the region of 745 – 830 cm^{-1}, the characteristic Fe – O magnetite bending (Fe^{+3} – O bound) were observed.

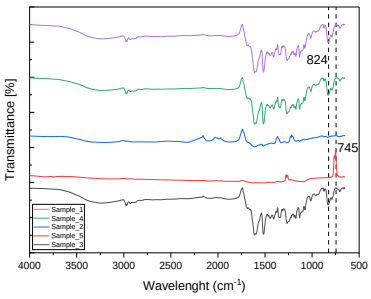

Fig.1. The FT-IR pattern of $Zn_{0.25}Fe_{2.75}O_4$ nanoparticles

To investigate crystal structure of the nanoparticles were analyzed by using Rigaku X-ray diffractometer, with CuK_α radiation (λ=0.154 nm). In Fig. 2 showed that the XRD patterns of samples synthesized at different hydrothermal conditions, respectively. All nanoparticles have the same characteristic (220), (311), (400), (422), (511) and (400) peaks of cubic spinel structure with cell constant a = 8.4 ± 0.01Å, which is good agreement with the value in the literature (JCPDS cad no. 89-1012, with a = 8.433 Å) [11]. There is no obvious impurity peak can be detected. In Fig. 2, to observe the effect of the reaction temperatures applied on the synthesized nanoparticles structure, the reaction time was kept approximately the same in Sample_2 and Sample_5 samples. It can be seen that the peak intensities decreased while the wideness of the peaks decreased as the reaction temperature increased with the same reaction time.

The average crystal size D (nm), of the $Zn_{0.25}Fe_{2.75}O_4$ nanoparticles were calculated from the highest intensity peak (311) using the Debye – Scherrer equation[5] and the presented in Table 2. The D (nm) of nanoparticles synthesized at 150°C and 180°C for 12 h were calculated to be 21 and 24 nm, respectively. The increase of the reaction temperature the nanoparticle size increased.

To analyze the effect of the reaction time on the nanoparticle size, as the reaction time was increased from 6 to 22 h at 150°C, the D (nm) increased from 14 to 20 nm, respectively. To get more detail of the investigation, at 180°C, the D (nm) of the nanoparticles synthesized for 3 and 12 h were found to be 23 and 25 nm, respectively. The D (nm) increased with increasing reaction time.

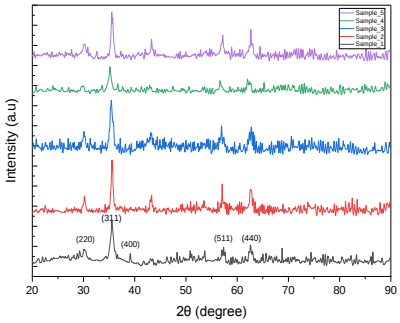

Fig.2. XRD patterns of $Zn_{0.25}Fe_{2.75}O_4$ nanoparticles

Using XRD data, the lattice parameter (*α*), crystal size (D), X-ray density (ρ), dislocation density (δ), and special surface area (S) of the samples were calculated using the following equations[12]. The results are presented in Table 2.

Table 2. Values of the D, α, ρ, δ, and S of the samples.

Sample No	D (nm)	α (nm)	ρ (g/cm^3)	δ ($10^{15} m^{-2}$)	S ($10^4 m^2/g$)
Sample_1	14.3	0.84	6.80	4.9	6.17
Sample_2	21.1	0.83	6.96	2.24	4.08
Sample_3	22	0.84	6.76	2.01	4.03
Sample_4	23	0.84	6.84	1.8	3.98
Sample_5	24	0.85	6.9	1.78	3.74

Since the crystal lattice parameter of magnetite is compatible with the literature for all three samples, the crystal structure of Fe_3O_4 is formed. When the structure is determined from the XRD pattern, we can also calculate the volume and mass of the cell, so that we can find the density of the sample.

The dislocation density (δ), defined as the length of the dislocation lines per unit volume of crystal[13], Sample_1 is 2 times higher than other samples. The surface area (S) is changed with reaction time and temperature.

The surface morphology of the nanoparticles was analyzed by scanning electron microscopy (SEM) using JEOL electron microscope 6700 coupled with EDX spectroscopy. SEM results show that all synthesized nanoparticles show a spherical shape. When reaction temperature was increased from 150° to 180°C, the crystallinity of nanoparticles increased. SEM microscopies of some samples are demonstrated in Fig. 3, respectively. The particle size increases with increasing reaction time and the surface morphology of the nanoparticles remains without change.

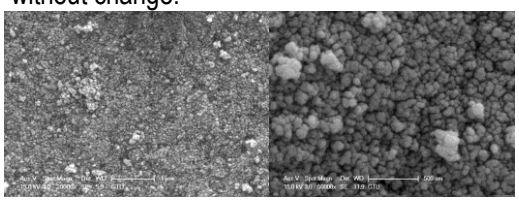

(a) **(b)**

Fig. 3. SEM images of nanoparticles (a) Sample_2 and (b) Sample_5.

The EDX spectrum of $Zn_{0.25}Fe_{2.75}O_4$ samples for different reaction temperature and time are shown in Figure 4. As can be seen, the spectrum confirms the presence of zinc dopant in Fe_3O_4. The spectrum recorded peak of the particles which show *Zn, Fe* and *O* related peaks. EDX analysis gives information about how much amount of *Zn* atom has really entered into the magnetite nanoparticles[14].

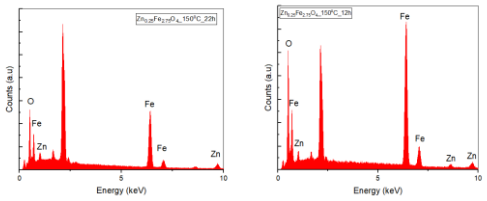

(a) **(b)**

Fig. 4. EDX spectra measured for nanoparticles of **(a)** Sample 2 and **(b)** Sample 5.

When reaction temperatures and times increased from 150°C to180°C and 3 h to 22; only 5.63% to 9.18% of *Zn* atoms have entered into magnetite. The first condition of the sample, it is seen that only 5.63% of *Zn* atoms entered into the structure and remaining *Zn* atoms could have been washed away[14]. Weight percentage (wt %) values of atoms are shown in Table 3. Elemental analysis approves that *Zn* element entered in the structures. EDX analysis approved that the nanoparticles are consisted of *Zn, Fe,* and *O* element. There is no other impurity.

Table 3. Values of elemental analysis of $Zn_{0.25}Fe_{2.75}O_4$ nanoparticles.

	Composition (wt%) Elements		
Sample No	Zn	Fe	O	Total
Sample_1	5.63	73.78	20.59	100
Sample_2	5.81	83.41	10.78	100
Sample_3	7.31	79.52	13.17	100
Sample_4	7.35	79.81	12.84	100
Sample_5	9.18	73.5	17.32	100

To determine the magnetic behavior of the samples, ESR analysis was first performed with Bruker EMX X-band Spectrometer and the Jeol Brand-JES-FA300 ESR Spectrometer[15]. The ESR patterns for all five samples are shown in Fig. 5.

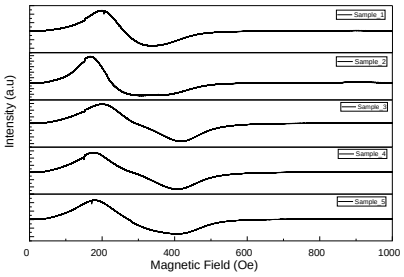

Fig 5. ESR spectra of samples

It is seen that all samples have unpaired electrons and all samples exhibit magnetic behavior. The sample of Sample_5 appears to have a larger ESR peak that the other samples.

Relaxation times of the synthesized samples; T_2, unpaired electron numbers; N_s, signal intensities from peak to peak; I_{pp}, full width half maximum; $\Delta H_{1/2}$, Lande factor; g and asymmetry factor; P_{asy} were calculated using the equations given below[16-19] All results of calculations are given in Table 4.

The resonance line width between two peaks is obtained from the FWHM value of the resonance spectrum.

The g value of the free electron is about 2. If the ratio of the magnetic moment to the angular moment of the system differs from that of the free electron, this difference comes from the spin-orbit match. Thus, the change in the value of g can also provide information about atomic or molecular orbitals containing unpaired electrons.

The resonance line width between two peaks is obtained from the FWHM value of the resonance spectrum. This width comes from the relaxation time of the excited electron. It was determined that when the crystal size increased, the T_2 value decreased.

Physical Properties Measurement System (PPMS) of Quantum Design Model 6000 device was used to get additional information about the magnetic properties of the synthesized $Zn_{0.25}Fe_{2.75}O_4$ structures.

All samples show super paramagnetic behavior, results are shown in Fig.6. The sample of Sample_3 has the highest saturation value. The main reason of it was the reaction time should have been long for 150°C. Except for this sample, the highest saturation value was obtained when the reaction time was 12h for 180°C which was named Sample_5. And the value was 89 emu/g. Besides, the highest remanent magnetization (M_r) value which is equal to 1 emu/g was observed in the Sample_5 sample. The lowest saturation magnetization value was observed in the

sample of Sample_1 with the smallest particle size in this experimental calculation.

Table 4. Values of g value, ΔH_{pp} , I_{pp} , N_s , T_2 , P_{asy} of the samples.

Sample No	g-value	ΔH_{pp} (mt)	I_{pp}	N_s	T_2 (10^{-11} s)	P_{asy}
Sample_1	2.50	144.46	4416.4	244.8	1.80	2.4
Sample_2	2.87	135.137	3528.4	183.7	1.67	3.1
Sample_3	2.20	218.878	5558.0	758.8	1.36	2.0
Sample_4	2.27	235.02	6098.4	960	1.22	2.6
Sample_5	2.39	227.9	4990	738.6	1.21	2.3

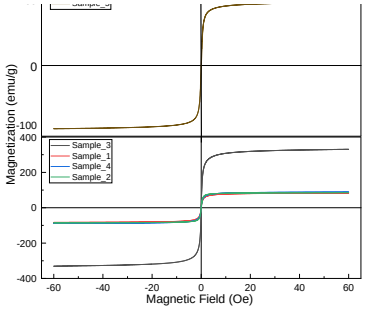

Fig 6. PPMS spectra of samples

Looking at these results, it was observed that the M_s results of samples in Table 5 are not overlap with the d_{XRD} (nm) results by calculated Scherrer's equation in Table 5. In literature doping of Zn, reduce the coercivity and also decrease the crystallite size, but increases the saturation magnetization[20].

Table 5. Table of PPMS parameter.

Sample No	Ms	Hc	Mr
Sample_1	83.2	24	1
Sample_2	85.6	65	9
Sample_3	331	2	0
Sample_4	88.3	14	1
Sample_5	89	0	1

Conclusions

In this study, $Zn_{0.25}Fe_{2.75}O_4$ nanoparticles are successfully prepared with an average crystallite size of 25 nm. It is showed a good monodispersity by hydrothermal method changing reaction conditions using NH_4OH as a base. It was approved that the hydrothermal conditions such as reaction temperature and time both had significant effects on structure and magnetic behaviour of nanoparticles. It was observed that the increase in reaction temperature caused increased the nanoparticle size. Besides, increased particle size affected magnetic analysis results, and saturation magnetization value decreasing with increasing particle size. Among different conditions, Sample_5 nanoparticles synthesized at 180°C for 12 h had good crystallinity and high saturation magnetization of 89 emu/g.

Acknowledgements

This project was supported by the Scientific and Technological Research Council of Turkey (TUBITAK Grant No: 115E776)

References

1. J.B. Mamani, A.J. Costa-Filho, D.R. Cornejo, E.D. Vieira, L.F. Gamarra, *J. Mater. Charact.* **81** (2013) 28-36.
2. An-Hui Lu, E.L. Salabas, F. Schuth, *Angew. Chem.* **46**(2007)1222-1244.
3. S. Laurent, D. Forge, M. Port, A. Roch, C. Robic, L. Vander Elst, R.N. Muller, *Chemical Reviews,* **108** (2008) 2064-2110
4. M. Ebrahimi, R.R. Shahraki, (2014) J Supercond Nov Magn
5. Atif, M., Hasanain, S.K. Nadeem, M, *Solid State Commun.* **81**, 563(1992)
6. Raeisi Shahraki, R., et al., *J. Magn. Magn. Mater.* **324**, 3762-3765(2012)

7. Tao, K., Dou, H., Sun, K., *Colloids Surf. A, Physicochem. Eng. Asp.* **320**, 115-122(2008)
8. Zhongping Chen, Metal-Organic, and Nano-Metal Chemistry 2012; 42(7) 1040-1046.
9. Habibi MH, Habibi AH, J Therm Anal Calorim. 2012
10. Caner Hasirci, Oznur Karaagac, Hakan Köçkar, Journal of Magnetism and Magnetic Materials, 2018.
11. T.J. Daou, G. Pourroy, S. Be´gin-Colin, J.M. Grene`che, C. Ulhaq-Bouillet, P. Legare, P. Bernhardt, C. Leuvrey, G. Rogez, *J. Chem. Mater.* **18**(2006) 4399-4404
12. Y. Köseoğlu, A. Baykal, M. S. Toprak, F. Gözüak, A.C.Başaran, B.Aktaş, *Journal of Alloys and Compounds* **462** (2008) 209-213.
13. G.K. Williamson, R.E.Smallman, Philosophical Magazine, 1:1, 34 (1956).
14. Chitra, M. Jay, K. Pushpanathan, and M. Loganathan, Materials and Manufacturing Processes, 2014.
15. Yoshio M, Eiichiro S, Kozo W. Springer-Verlag Berlin Heidelberg, 2011
16. Kundu, A., Upadhyay, C., Verma, H., *Phys. Lett. A* **311**, 410-415 (2003)
17. J. Al Boukhari, L. Zeidan, A. Khalaf, R. Awad, *Chemical Physics* 2019; **516**: 116-124.
18. Adil G., *Applied Ceramic Technology* 2019; **00**:1-8.
19. Bernice GS, Michael K, George KF., The *Journal of Chemical Physics* 1965; **43**(12):4191.
20. F. Salehpour, A Khorramdin, H. Shokrollahi, A. Pezeshki, F. Mirzaei, N.D. Nader, *Journal of Nanotechnology in Engineering and Medicine* 2014